Ther Adv Neurol Disord
2021, Vol. 14: 1–13
DOI: 10.1177/17562864211029551

Prediction of the progression from mild cognitive impairment to Alzheimer's disease using a radiomics-integrated model

Zhen-Yu Shu#, De-Wang Mao#, Yu-yun Xu, Yuan Shao, Pei-Pei Pang and Xiang-Yang Gong

Abstract

Objective: This study aimed to build and validate a radiomics-integrated model with whole-brain magnetic resonance imaging (MRI) to predict the progression of mild cognitive impairment (MCI) to Alzheimer's disease (AD).

Methods: 357 patients with MCI were selected from the ADNI database, which is an open-source database for AD with multicentre cooperation, of which 154 progressed to AD during the 48-month follow-up period. Subjects were divided into a training and test group. For each patient, the baseline T_1WI MR images were automatically segmented into white matter, gray matter and cerebrospinal fluid (CSF), and radiomics features were extracted from each tissue. Based on the data from the training group, a radiomics signature was built using logistic regression after dimensionality reduction. The radiomics signatures, in combination with the apolipoprotein E4 (APOE4) and baseline neuropsychological scales, were used to build an integrated model using machine learning. The receiver operating characteristics (ROC) curve and data of the test group were used to evaluate the diagnostic accuracy and reliability of the model, respectively. In addition, the clinical prognostic efficacy of the model was evaluated based on the time of progression from MCI to AD.

Results: Stepwise logistic regression analysis showed that the APOE4, clinical dementia rating, AD assessment scale, and radiomics signature were independent predictors of MCI progression to AD. The integrated model was constructed based on independent predictors using machine learning. The ROC curve showed that the accuracy of the model in the training and the test sets was 0.814 and 0.807, with a specificity of 0.671 and 0.738, and a sensitivity of 0.822 and 0.745, respectively. In addition, the model had the most significant diagnostic efficacy in predicting MCI progression to AD within 12 months, with an AUC of 0.814, sensitivity of 0.726, and specificity of 0.798.

Conclusion: The integrated model based on whole-brain radiomics can accurately identify and predict the high-risk population of MCI patients who may progress to AD. Radiomics biomarkers are practical in the precursory stage of such disease.

Keywords: Alzheimer's disease, machine learning, magnetic resonance imaging, mild cognitive impairment, radiomics

Received: 13 February 2021; revised manuscript accepted: 7 June 2021.

Correspondence to:
Xiang-Yang Gong
Department of Radiology, Zhejiang Provincial People's Hospital, Affiliated People's Hospital of Hangzhou Medical College, Hangzhou, 310014, China
cjr.gxy@hotmail.com

Zhen-Yu Shu
De-Wang Mao
Yu-yun Xu
Yuan Shao
Xiang-Yang Gong
Department of Radiology, Zhejiang Provincial People's Hospital, People's Hospital of Hangzhou Medical College, Hangzhou, China

Pei-Pei Pang
GE Healthcare China, Shanghai, China

#These authors have contributed equally to this work.

Introduction

Alzheimer's disease (AD) is a progressive neurodegenerative disease with high morbidity.[1] To date, there is no single treatment that can stop or reverse the progression of AD. Mild cognitive impairment (MCI), a transitional state between normal ageing and dementia, has been identified as a high risk factor for AD. Epidemiological studies have indicated that approximately 10–12% of patients with MCI progress to AD each

year.[2] Since many elderly individuals have MCI, but do not meet the diagnostic criteria for AD, early intervention for individuals at this stage may effectively delay progression of the disease.[3]

MCI does not affect daily activities, and individuals with MCI have normal cognitive function.[4] However, MCI exhibits heterogeneous features in cognitive function and clinical progression, and the clinical outcomes remain uncertain. Some MCI patients remain stable, or even revert to normal functions, whereas others progress towards AD.[5] Therefore, there is an urgent need to define biomarkers that can identify and predict high-risk individuals with MCI who will progress to AD, as these individuals will require subsequent intervention. Currently, biochemical changes in the cerebrospinal fluid (CSF) and neuroimaging measures of brain anatomy and function have been identified as reliable biomarkers of AD.[6–8] Such features include increased CSF tau, hypometabolism in the posterior cingulate, and hippocampal atrophy.[9,10] Using a machine-learning model with the combined use of these biomarkers, the automatic diagnosis and prognosis of AD patients has been proven to be reliable and highly accurate.[11] However, the applicability of these biomarkers may be limited due to the high prevalence of AD, high cost of these techniques, and their relative difficulty of use.

Radiomics is a new approach based on the deep cross-fusing of medicine and computer science. It reflects the heterogeneity of disease through image features and has the characteristics of being low cost and non-invasive.[12,13] In the early years, this new method was widely used in oncology,[14] and radiomics has now been used in the diagnosis and categorical assessment of MCI and AD.[15] In the past few years, neuroimaging studies have shown that white matter (WM) degeneration and demyelination in the microscopic and macroscopic structure of WM are important physiological features in the identification of risk and progression of AD.[16] These microstructural changes can be identified in three-dimensional whole-brain WM radiomics analyses.[17] In addition, grey matter (GM) atrophy and pathological changes in the CSF can identify very early changes associated with pathological ageing and AD.[18] As a result, we hypothesize that whole-brain GM and CSF radiomics analysis may explain the heterogeneity of brain tissue in patients with MCI. We further believe that a whole-brain-based radiological approach may be more powerful than single region analysis in accurately identifying patients who may progress to AD.

Since AD is a complex neurodegenerative disorder, it is clear that a single marker cannot accurately diagnose AD and monitor disease progression.[19] However, radiomics, in combination with clinical data and gene data, can be used to establish a disease prediction model to improve the prediction accuracy.[20,21] In addition, it is known that the E4 allele of the apolipoprotein (APOE4) is the major known genetic risk factor for late-onset AD.[22] The addition of APOE4 and neuropsychological scale data analysis can improve the diagnosis of MCI.[23,24] Therefore, a combination of different markers may provide a more comprehensive approach for the early diagnosis and monitoring of AD.

This study aimed to identify possible novel whole-brain biomarkers with radiomics using conventional magnetic resonance imaging (MRI) techniques, and to develop an integrated model using radiomics in combination with genetic traits and neuropsychological scales. This approach was used to identified individuals with MCI at high risk of progressing to AD. This radiomics-integrated model may be helpful to develop individualized and accurate medical plans in clinical practice.

Materials and methods

Patient information

Our study did not require an ethical board approval because all the original data used in this study, including neuropsychological scales, MRI and genetic data, were obtained from the Alzheimer's disease neuroimaging initiative (ADNI) project (ADNI.Loni.USC.EDU), an open-source database for AD with multicentre cooperation. The ADNI project aims to comprehensively evaluate the progress of MCI and early AD through the combination of longitudinal MRI, positron emission tomography (PET), and biomarker data, as well as clinical neuropsychological scale assessments. In addition, the project is committed to finding biomarkers for the diagnosis and prognosis of AD, and to developing potential biomarkers for clinical application. In the present study, we selected 357 patients with MCI, who were followed up for 4 years with complete clinical data, including baseline MRI, genetic data, and

neuropsychological data such as the Mini-Mental State Examination (MMSE), Clinical Dementia Rating (CDR), and the Alzheimer's Disease Assessment Scale (ADAS). Of the 357 patients, 154 patients progressed to AD within 4 years. In addition, according to the original ADNI participant number, these patients were assigned to a training set ($n = 249$) or a test set ($n = 108$) at a 7:3 ratio. The prediction model was established using the training set, and the reliability of the model was verified using the test set.

Image preprocessing

The T1-weighted images (T1WI) were imported into the SPM12 software (https://www.fil.ion.ucl.ac.uk/spm/software/spm12/), and DICOM data were automatically segmented into whole-brain WM, GM, and CSF. The correctness of the automatic segmentation was confirmed by two experienced neuro-radiologists with 6–10 years of neuroimaging experience, and if needed, were manually modified (WM, GM, and CSF volumes) using the ITK-SNAP software (http://www.itksnap.org). The two neuro-radiologists were blinded to the clinical data. The modification was performed by removing non-brain tissue, brainstem, and cerebellum, and correcting segmentation errors in brain tissues. After manual correction, the brain tissues were imported into the QK software (Quantitative Analysis Kit, version 1.2, GE Healthcare) for feature extraction. Before feature extraction, image preprocessing was performed as previously described.[25] Briefly, T1WI data were resampled at a resolution of $1 \times 1 \times 1\,mm^3$ voxel size using linear interpolation. To reduce image noise, the image greyscale intensity level was discretized and normalized by downsampling each image into 32 bins, thus resulting in an image grey range with equally spaced intervals. Therefore, the bin size and intensity resolution of the discretized volumes depended on the greyscale value (i.e. four bin sizes for each greyscale).

Radiomics feature extraction and selection

The IPM software package of the QK analysis platform was used to extract the radiomics features, including the histogram, Haralick, grey level co-occurrence matrix (GLCM), run length matrix (RLM), and grey level size zone matrix (GLZSM) features. Only the features that were most consistent across different radiologists were selected to ensure robustness. The Spearman rank correlation test was used to calculate the correlation coefficient between feature set A (from radiologist A) and feature set B (from radiologist B). Robust features were defined as those that exhibited a correlation coefficient greater than 0.8.[26] To prevent the 'curse of dimensionality' caused by too many features, which can lead to inaccurate prediction results,[27] the dimension of the extracted features was reduced using the maximum relevance minimum redundancy (mRMR) algorithm and traditional least absolute shrinkage and selection operator (LASSO) algorithm. The mRMR algorithm selects a group of features, which can be divided into two categories (stable and progression) to the greatest extent and with minimum intracorrelation of features.[28,29] The traditional LASSO algorithm was used to further reduce the dimensionality of the selected features to generate a final set of top-level radiation features related to MCI progression,[30] and to participate in the construction of the radiomics signature.

After feature dimensionality reduction of the training set, a joint feature set containing WM, GM, and CSF was obtained, and the radiomics signature was constructed using multivariate logistic regression. The ability of the signature to predict MCI conversion to AD was evaluated using the rad scores calculated based on the radiomics signature formula. Each patient in the training set was assigned a score that reflected the conversion probability of MCI to AD. The rad score of the test set was calculated by the signature formula of the training set. The area under the curve (AUC) of the receiver operating characteristic (ROC) curve was used to evaluate the accuracy of the radiomics signature in the training and test sets. The radiomics signature formula can be found in the Supplementary Materials.

Construction of the integrated model

A backward stepwise selection method with a stopping rule based on Akaike's information criterion (AIC) was conducted to select potential predictors in the training set, including demographic characteristics, genetic data, neuropsychological scales, and radiomics signatures. Multiple regression analysis was used to obtain the final predictive factors used for integrated model construction. The variance inflation factor (VIF) was used to diagnose the collinearity of each variable with VIF values, with VIF values greater than 10 indicated

Table 1. Characteristics of patients in the training and test sets.

Variable	Training set ($n = 249$)	Test set ($n = 108$)	p-value
Age (years)	74.2 (7.8)	75.3 (7.3)	0. 15
APOE4 [*n* (%)]			
No	119 (47.8)	48 (44.4)	0.641
Yes	130 (52.2)	60 (55.6)	
Gender [*n* (%)]			
Male	156 (62.7)	73 (67.6)	0.438
Female	93 (37.3)	35 (32.4)	
Education (years)	15.7 (3)	15.6 (2.8)	0.859
CDR (score)	1.6 (0.9)	1.6 (0.9)	0.637
ADAS (score)	11.5 (4.3)	11.9 (4.8)	0.471
MMSE (score)	26.9 (1.8)	27.2 (1.8)	0.106

ADAS, Alzheimer's disease assessment scale; APOE4, apolipoprotein E 4; CDR, clinical dementia rating scale; MMSE, mini-mental state examination.

severe multicollinearity.[31] Machine-learning classification algorithms exhibit a strong ability to recognize neurodegeneration (e.g. AD and MCI).[32,33] Support vector machines (SVMs) in particular can provide a comprehensive way to characterize the whole spatial dimension. Accordingly, SVM was used to construct the prediction model based on the filtered prediction factors, and then the test set data was used to calculate the predictive efficiency based on the predictive model. In this study, an SVM classifier was developed using the MATLAB platform (version 8.3.0.532). An SVM algorithm with a radial basis kernel was applied to construct classification models. The performance of each model was validated using the training and test sets, using diagnostic accuracy, calibration performance, and net benefit as evaluation metrics. These metrics were evaluated using ROC curve analysis, calibration curve analysis, and decision curve analysis (DCA), respectively. In addition, to further quantify the performance of the model, an ROC curve was used to evaluate the diagnostic performance of the integrated model and each predictor. The Delong test was used to measure the differences in the ROC curves between the joint model and the predictors. At last, we predicted the population disease progression at different transformation times to clarify the model's clinical efficacy.

Statistical analysis

Statistical analyses were performed using the SPSS software 17.0 (IBM, Armonk, NY), GraphPad (San Diego, CA), and R software (version 3.4.1; http://www.Rproject.org). The Kolmogorov–Smirnov test was used to evaluate the normality of variable distributions. For data with a normal distribution, a Student's *t*-test was used to evaluate the differences between groups. For data without a normal distribution, a Mann–Whitney test was used. For categorical data, a chi-squared test was used to evaluate differences between groups. The 'rms' package of R software was used to construct the plot of calibration. Statistical significance was considered as $p < 0.05$.

Results

Clinical characteristics of the patients

Table 1 summarizes the clinical characteristics of patients in the training and test sets. There were no significant differences in age, APOE4, gender, education, CDR, scores, ADAS scores, and MMSE scores between the training and the test sets. In the training set, the APOE4, CDR scores, ADAS scores, MMSE scores, and radiomics signature scores were significantly different between the stable and transformed group (Table 2). In the test set, the CDR scores, ADAS scores, MMSE scores, and radiomics signature scores were significantly different between the stable and transformed groups (all $p < 0.05$) (Table 2). The other factors were not significantly different between groups.

The establishment and evaluation of the radiomics signature

Figure 1 shows the radiomics workflow. A total of 378 radiomic features were extracted from each brain tissue (WM, GM, CSF), indicating that for each patient, 1134 features were extracted from the T1WI images. Among these features, 10 features, including three from WM, three from GM, and four from CSF, were retained after feature dimensionality reduction. Finally, logistic regression was used to construct the radiomics signature. The rad scores were significantly different between the training and test sets. The ROC curve showed that the prediction performance of the radiomics signature in the training and test sets was good, with AUC values of 0.722 and 0.692, specificity values of 0.697 and 0.721, and

Table 2. Clinical characteristics of patients with and without MCI progression in the training and test sets.

Variable	Training set (*n* = 249)			Test set (*n* = 108)		
	Stable (*n* = 142)	Progression (*n* = 107)	*p*-value	Stable (*n* = 61)	Progression (*n* = 47)	*p*-value
Age (years)	75.5 (7.5)	75 (7)	0.569	72.8 (8.2)	73.8 (7.4)	0.484
APOE4 [*n* (%)]						
No	84 (59.2)	35 (32.7)	<0.001*	32 (52.5)	16 (34)	0.0864
Yes	58 (40.8)	72 (67.3)		29 (47.5)	31 (66)	
Sex [*n* (%)]						
Male	95 (66.9)	61 (57)	0.142	39 (63.9)	34 (72.3)	0.472
Female	47 (33.1)	46 (43)		22 (36.1)	13 (27.7)	
Education(years)	15.5 (3)	16 (2.9)	0.166	15.7 (3)	15.6 (2.5)	0.781
CDR (score)	1.4 (0.8)	1.9 (0.9)	<0.001*	1.5 (0.7)	1.8 (1)	0.023*
ADAS (score)	10.3 (4.3)	13.1 (3.8)	<0.001*	10.4 (4.3	13.7 (4.8)	<0.001*
MMSE (score)	27.2 (1.8)	26.4 (1.6)	<0.001*	27.5 (1.8)	26.9 (1.7)	0.048*
Radiomics signature (score)	−0.7 (1.1)	0.1 (0.7)	<0.001*	−0.8 (0.9)	−0.3 (0.8)	0.002*

*$p < 0.05$.
ADAS, Alzheimer's disease assessment scale; APOE4, apolipoprotein E 4; CDR, clinical dementia rating scale; MCI, mild cognitive impairment; MMSE, mini-mental state examination.

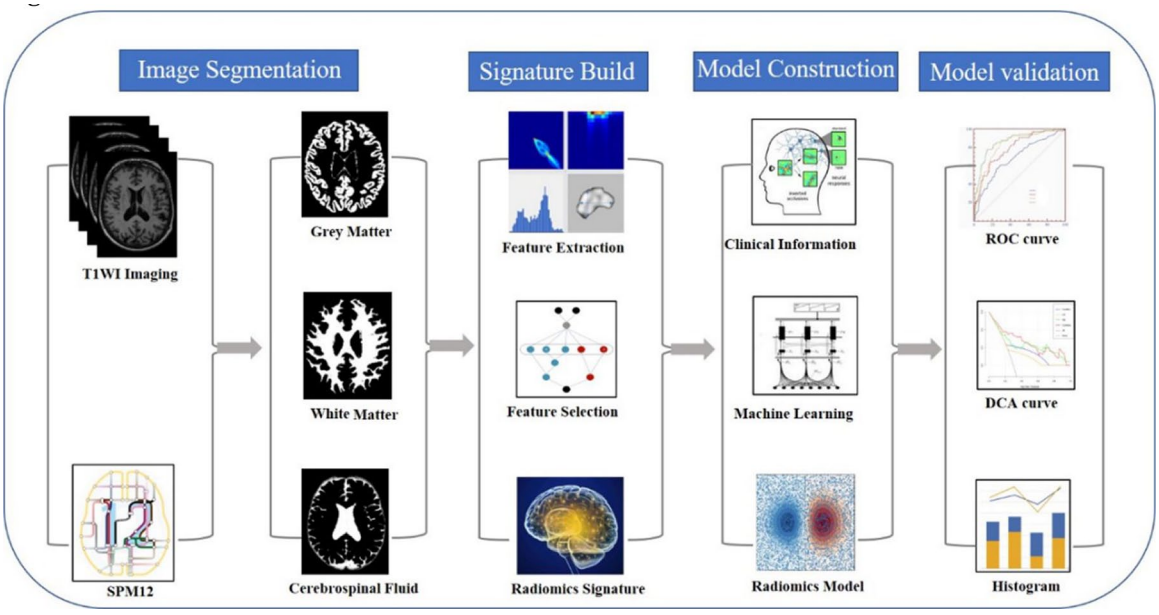

Figure 1. The construction process of the integrated model.

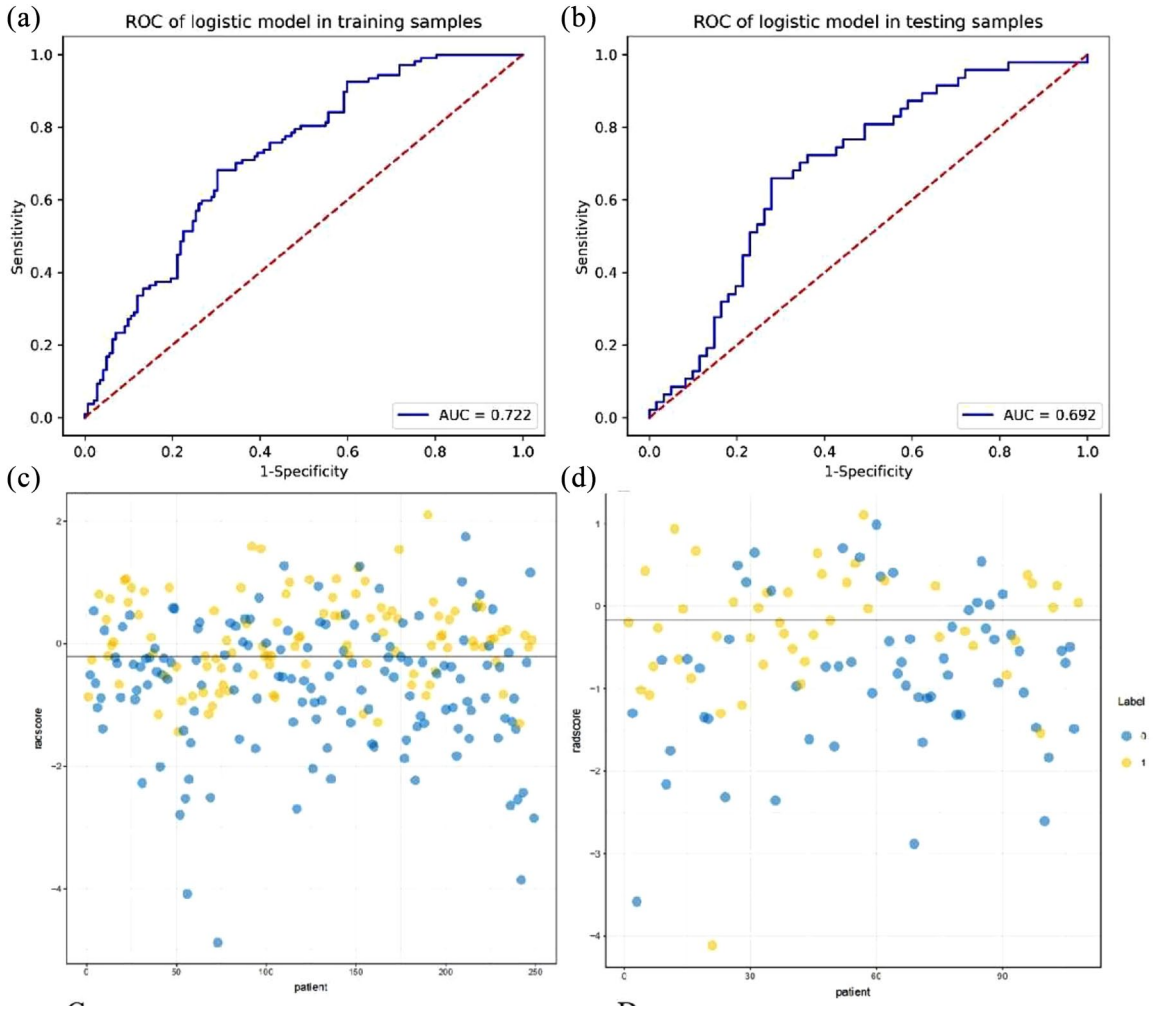

Figure 2. Score diagrams of the radiomics signature in the training set (a) and the test (b) set. The diagnostic accuracy of the rad score of the radiomics signature in the training (c) and test (d) sets. The blue dots indicate disease stability, and the yellow dots indicate progression.

sensitivity values of 0.682 and 0.659, respectively (Figure 2). The detailed results and process of dimensionality reduction are shown in the Supplementary Materials.

Construction and performance evaluation of the integrated model

Based on stepwise logistic regression analysis, APOE4, CDR scores, ADAS scores, and radiomics signature scores were independent predictors for MCI conversion to AD. VIF values of APOE4, CDR scores, ADAS scores, and radiomics signature scores were 1.048, 1.04, 1.107, and 1.051, respectively, suggesting that there were no severe collinearities in these factors (see Table 3). The SVM was used to construct an integrated model based on independent prediction factors. The ROC curve showed that the accuracy of the integrated model, radiomics signature, ADAS scores, CDR scores, and APOE4 in the training set was 0.814, 0.722, 0.696, 0.657, and 0.632, respectively with a specificity of 0.671, 0.697, 0.748, 0.747, and 0.592, and a sensitivity of 0.822, 0.682, 0.563, 0.514, and 0.673, respectively. The ROC curve showed that the accuracy of the integrated model, radiomics signature, ADAS scores, CDR scores, and APOE4 in the test set was 0.807, 0.692, 0.695, 0.599, and 0.592, with a specificity of 0.738, 0.721, 0.803, 0.672, and 0.525 and a sensitivity of 0.745, 0.659, 0.532, 0.511, and 0.66, respectively (Figure 3). Furthermore, the Delong test demonstrated that the performance of the integrated model was significantly higher compared to the other

Table 3. Screening of predictors involved in the integrated model construction.

Variable	Multivariate logistic regression		
	OR (95% CI)	*p*-value	VIF value
Age	0.979 (0.937–1.023)	0.346	NA
APOE4	2.513 (1.376–4.589)	0.003*	1.048
Sex	1.301 (0.684–2.474)	0.423	NA
Education	1.089 (0.98–1.211)	0.114	NA
CDR	1.856 (1.285–2.68)	0.001*	1.04
ADAS	1.116 (1.036–1.201)	0.004*	1.107
MMSE	0.855 (0.708–1.033)	0.114	NA
Radiomics signature	2.575 (1.75–3.79)	<0.001*	1.051

*$p < 0.05$.
ADAS, Alzheimer's disease assessment scale; APOE4, apolipoprotein E4; CDR, clinical dementia rating scale; CI, confidence interval; VIF, variance inflation factor; MMSE, mini-mental state examination; OR, odd's ratio.

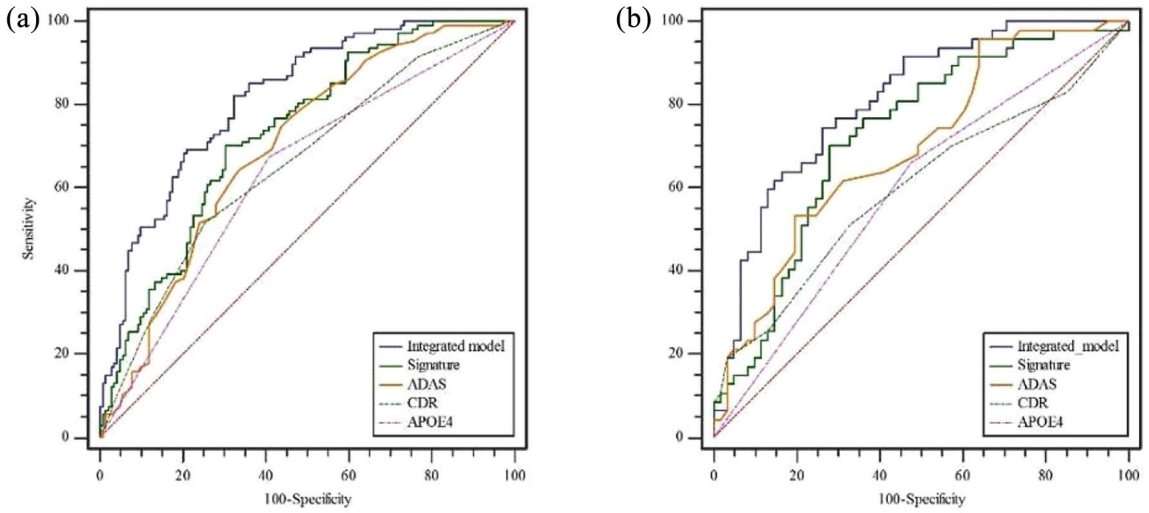

Figure 3. ROC curves for the integrated model, radiomics signature scores, ADAS scores, CDR scores and APOE4 for the prediction of progression from MCI to AD in the training (a) and test (b) sets.
AD, Alzheimer's disease; ADAS, Alzheimer's disease assessment scale; APOE4, apolipoprotein E4; CDR, clinical dementia rating scale; MCI, mild cognitive impairment.

independent predictors in the training and test sets ($p < 0.05$).

Overall validation of the integrated model

We performed DCA on the integrated model, radiomics signature, ADAS scores, CDR scores, and APOE4 in the training and test sets. The integrated model had the greatest net benefit in both datasets. The calibration curve was used to analyze the continuous variables, including the model, radiomics signature, ADAS scores, and CDR scores in the two datasets, which showed good consistency (Figure 4). The probability score of each patient's conversion to AD was calculated based on the integrated model. In the training and test sets, the scores were significantly higher in the progression group compared with the stable group

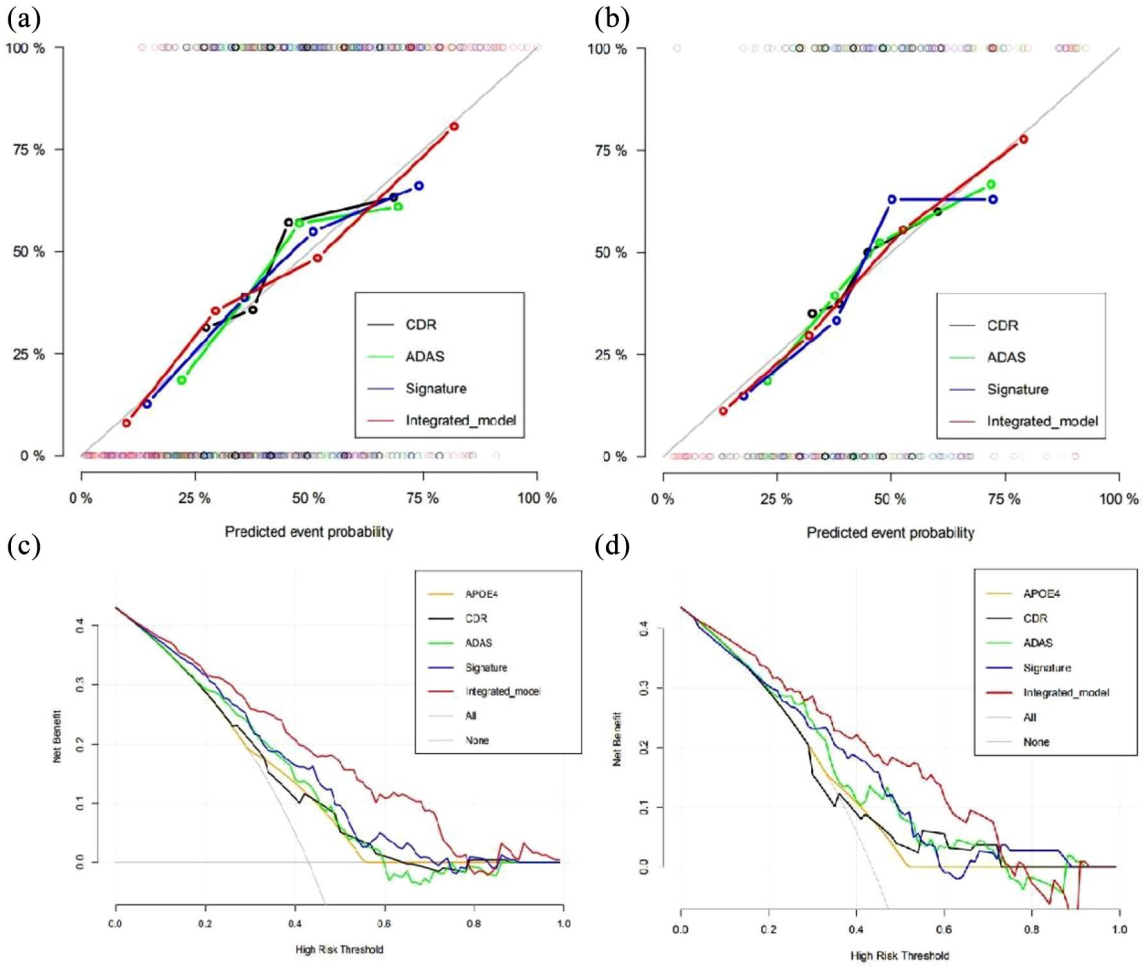

Figure 4. Calibration curves for the integrated model, radiomics signature, ADAS scores, and CDR scores for the prediction of progression from MCI to AD in the training (a) and test (b) sets. DCA curves for the associative integrated models, signature, ADAS scores, CDR scores and APOE4 in the training (c) and test (d) sets.
AD, Alzheimer's disease; ADAS, Alzheimer's disease assessment scale; APOE4, apolipoprotein E4; CDR, clinical dementia rating scale; MCI, mild cognitive impairment.

(Figure 5). The ROC curve was used to study the diagnostic accuracy based on the conversion time and showed that the prediction of 1-year MCI conversion to AD by the model had the maximum diagnostic efficacy (Table 4).

Discussion

In this study, we used WM, GM, and CSF volumes to build a radiomics signature. We found that, the rad score was significantly different between stable MCI patients and progression MCI patients, suggesting that a whole-brain-based radiomics signature can be used as a potential biomarker to identify patients who progress from MCI to AD. In addition, the integrated model, with the use of the radiomic signature and genetic and neuropsychological scale data, showed that the time point for the greatest predicting efficacy from MCI to AD was 1 year. The radiomics-integrated model may provide a reliable tool in clinical practice to identify high-risk patients with MCI who may progress to AD.

Biomarkers play a major role in the early diagnosis and prediction of AD.[34] The most studied biomarkers include neuropsychological markers, biochemical markers, and neuroimaging markers.[35] However, the clinical application of biochemical markers is poor, and neuropsychological markers are more subjective and can be applied only to patients with clinical symptoms. Therefore,

Table 4. Performance evaluation of the integrated model at different time points.

Time	Receiver operating characteristic curve		
	AUC	Sensitivity	Specificity
6 months	0.774	0.619	0.817
12 months	0.814	0.726	0.798
18 months	0.81	0.692	0.798
24 months	0.794	0.672	0.798
36 months	0.797	0.787	0.685
48 months	0.742	0.75	0.82

AUC, area under the curve.

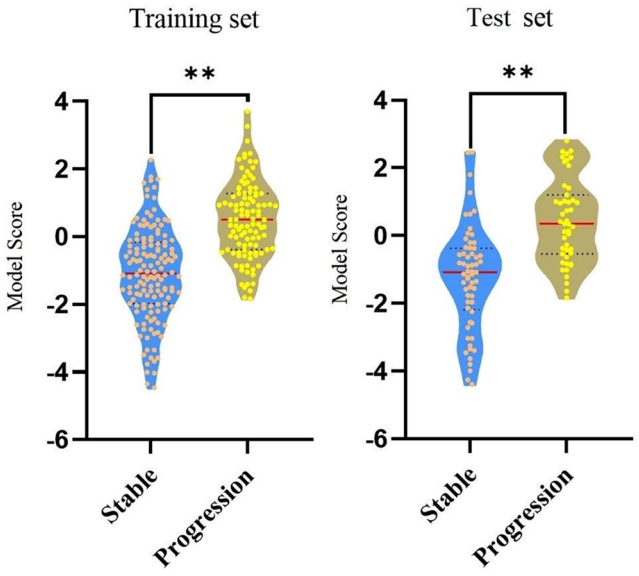

Figure 5. Violin box diagram of the model score. Statistically significant differences in model scores were observed between the stable and progression groups in the training (left) and test (right) sets.
**Denotes $p < 0.001$, the red line denotes the median, and the black dotted line denotes the first and third quartiles.

neuroimaging markers are currently the main research focus, and MRI, which reflects brain tissue structure non-invasively and intuitively, has become an important factor in neuroimaging research.[36–38] The volume of the hippocampus and the thickness of the cortex have been widely used in the study of the evolution of AD.[39,40] However, these brain regions reflect only the local pathological mechanism of the disease, but not the pathological changes in the evolution of MCI to AD. In this study, we developed a novel whole-brain biomarker based on radiomics analysis to identify the high-risk population of MCI patients who may progress to AD. Our results showed that the radiomics signature had good diagnostic efficiency, which may reflect most of the pathological changes that take place during disease progression. This is likely due to the fact that radiomics features of the signature obtained from the WM, GM, and CSF are closely related to the conversion of MCI to AD.[41] In addition, most of the radiomics features of the signatures belong to high-level disease attributes. For example, it has been reported that RLM features are related to WM damage,[42] which plays an important role in the transformation of MCI to AD. In addition, the complexity and roughness derived from GLCM features can reflect the degree of association between different pixels in the same brain region. Therefore, GLCM features involved in the construction of signatures indicate that brain structural damage may lead to changes in the complexity and distribution of voxels in disease-relevant regions. A previous study by Feng *et al.*[43] supports this idea,[15] further confirming the prognostic value of high-price quantitative image features in neurodegenerative diseases. Furthermore, previous similar studies have shown that structural atrophy and functional metabolic abnormalities related to MCI progression were mainly in brain areas such as the hippocampus, frontal lobe, and temporal cortex.[44] Therefore, our study may further expand the scope of radiomics studies in brain regions affected by neurodegenerative diseases.

Biomarkers can be used to track disease progression over time when studying the effectiveness of new modification therapies for AD.[45] Many methods such as amyloid imaging, functional MRI, and F-deoxyglucose positron emission tomography (PET) can be used to predict the potential progress of AD.[46–49] However, a single marker is unlikely to completely describe the status and progression of AD. Given the lack of ideal diagnostic methods, a combination of biomarkers may improve the diagnostic accuracy of AD.[50] Our results also confirm this idea, in that our prediction model significantly improved the diagnostic efficiency by the combined use of a radiomics signature, APOE4, and neuropsychological scales. The predictive accuracy of MCI progression obtained by the current combined markers method is very similar to that of previous SPECT studies. In fact, the diagnostic efficiency of

SPECT in predicting AD conversion in patients with MCI ranged from 0.74 to 0.82,[51] which were similar to the results of this study. Further studies are required to assess whether the combination of whole-brain biomarkers and other brain imaging methods will lead to better risk assessment and diagnosis.

Chen *et al.*[52] used the CARE index, which combines multiple dimensions of biomarkers, including cognition, CSF, a GM concentration index, and a hippocampal functional connectivity index, to predict the progress of MCI, and showed a high diagnostic efficiency (AUC = 0.861). However, considering the small sample size (n = 102 patients) in their study, our results may be more valuable for evaluating MCI progression. In addition, our results also showed that the diagnostic efficiency of the integrated model was the highest for predicting one-year conversion to AD (AUC = 0.814). Nevertheless, the diagnostic efficiency in our case was lower than that reported by Minhas *et al.*,[53] which found a one-year conversion accuracy to AD of 0.88 based on the longitudinal integrated index of MRI. The integrated index includes MRI biomarkers, such as the volume, surface area, and cortical thickness of different brain regions, in addition to a variety of neuropsychological indicators, such as the ADAS and MMSE. However, since approximately 50–80% of MCI patients do not progress to AD during the follow-up period of 3–4 years, the cost of assessment will be greatly increased when using this method to confirm such progression.[54] In such a heterogeneous population, long-term follow-up of these biomarkers may be more difficult, and will lead to a heavier burden of medical resources. In addition, our study used APOE4 genetic data for predicting MCI progression to AD. Although additional tests for APOE genetic information increases the cost for the patients, only one test at the beginning of the follow-up period is necessary to build the prediction model. As a result, our model provides a non-invasive and convenient approach for screening early AD in the clinic.

Our study also has some limitations. Firstly, this study used a relatively short follow-up period. A certain proportion of currently stable patients may progress to AD later in life. However, the proportion of MCI patients who progress to AD is uncertain. AD progression is higher during the first few years of follow-up, but decreases during longer follow-up intervals.[55] Secondly, this study is a retrospective study based on information available in public databases. It is necessary to conduct further longitudinal prospective studies on MCI patients to confirm the results of this study.

In summary, this study found that whole-brain-based radiomics biomarkers can be used to identify high-risk patients with MCI who may convert to AD in the future. In addition, radiomics biomarkers in combination with genetic data and neuropsychological scale analysis can significantly improve the predictive performance of MCI to AD.

Author contributions

Xiangyang Gong and Zhenyu Shu contributed to the conception and design of the study.

Yuyun Xu and Yuan Shao provided and prepared the samples.

Yuyun Xu and Dewang Mao reconstructed and analyzed the images.

Zhenyu Shu, and Peipei Pang analyzed and interpreted the data.

Zhenyu Shu wrote the manuscript with input from all authors.

Conflict of interest statement

Peipei Pang was employed by the company GE Healthcare. The other authors declare that the research was conducted in the absence of any commercial or financial relationships that could be construed as a potential conflict of interest.

Funding

The authors disclosed receipt of the following financial support for the research, authorship, and/or publication of this article: Fund of Health Commission of Zhejiang Province in China, Grant/Award Number: 2020KY039.

ORCID iD

Zhen-Yu Shu https://orcid.org/0000-0002-7529-2357

Supplemental material

Supplemental material for this article is available online.

Reference

1. Lane CA, Hardy J and Schott JM. Alzheimer's disease. *Eur J Neurol* 2018; 25: 59–70.

2. Langa KM and Levine DA. The diagnosis and management of mild cognitive impairment: a clinical review. *JAMA* 2014; 312: 2551–2561.
3. Jack CR Jr, Knopman DS, Jagust WJ, *et al.* Tracking pathophysiological processes in Alzheimer's disease: an updated hypothetical model of dynamic biomarkers. *Lancet Neurol* 2013; 12: 207–216.
4. Vega JN and Newhouse PA. Mild cognitive impairment: diagnosis, longitudinal course, and emerging treatments. *Curr Psychiatry Rep* 2014; 16: 490.
5. Gauthier S, Reisberg B, Zaudig M, *et al.* Mild cognitive impairment. *Lancet* 2006; 367: 1262–1270.
6. Da X, Toledo JB, Zee J, *et al.* Integration and relative value of biomarkers for prediction of MCI to AD progression: spatial patterns of brain atrophy, cognitive scores, APOE genotype and CSF biomarkers. *NeuroImage Clin* 2013; 4: 164–173.
7. Dickerson BC, Wolk DA and Alzheimer's Disease Neuroimaging Initiative. Biomarker-based prediction of progression in MCI: comparison of AD signature and hippocampal volume with spinal fluid amyloid-β and tau. *Front Aging Neurosci* 2013; 5: 55.
8. Salvatore C, Cerasa A and Castiglioni I. MRI characterizes the progressive course of AD and predicts conversion to Alzheimer's dementia 24 months before probable diagnosis. *Front Aging Neurosci* 2018; 10: 135.
9. Geuze E, Vermetten E and Bremner JD. MR-based in vivo hippocampal volumetrics: 2. Findings in neuropsychological disorders. *Mol Psychiatry* 2005; 10: 160–184.
10. Sperling RA, Aisen PS, Beckett LA, *et al.* Toward defining the preclinical stages of Alzheimer's disease: recommendations from the National Institute on Aging-Alzheimer's Association workgroups on diagnostic guidelines for Alzheimer's disease. *Alzheimers Dement* 2011; 7: 280–292.
11. Salvatore C, Battista P and Castiglioni I. Frontiers for the early diagnosis of AD by means of MRI brain imaging and support vector machines. *Curr Alzheimer Res* 2016; 13: 509–533.
12. Yip SS and Aerts HJ. Applications and limitations of radiomics. *Phys Med Biol* 2016; 61: R150–R166.
13. Lambin P, Leijenaar RTH, Deist TM, *et al.* Radiomics: the bridge between medical imaging and personalized medicine. *Nat Rev Clin Oncol* 2017; 14: 749–762.
14. Gillies RJ, Kinahan PE and Hricak H. Radiomics: images are more than pictures, they are data. *Radiology* 2016; 278: 563–577.
15. Qi F and Ding Z. MRI radiomics classification and prediction in Alzheimer's disease and mild cognitive impairment: a review. *Curr Alzheimer Res* 2020; 17: 297–309.
16. Nasrabady SE, Rizvi B, Goldman JE, *et al.* White matter changes in Alzheimer's disease: a focus on myelin and oligodendrocytes. *Acta Neuropathol Commun* 2018; 6: 22.
17. Shao Y, Chen Z, Ming S, *et al.* Predicting the development of normal-appearing white matter with radiomics in the aging brain: a longitudinal clinical study. *Front Aging Neurosci* 2018; 10: 393.
18. Jack CR Jr, Bennett DA, Blennow K, *et al.* NIA-AA research framework: toward a biological definition of Alzheimer's disease. *Alzheimers Dement* 2018; 14: 535–562.
19. Blennow K and Zetterberg H. Biomarkers for Alzheimer's disease: current status and prospects for the future. *J Intern Med* 2018; 284: 643–663.
20. Kumar V, Gu Y, Basu S, *et al.* Radiomics: the process and the challenges. *Magn Reson Imaging* 2012; 30: 1234–1248.
21. Thawani R, McLane M, Beig N, *et al.* Radiomics and radiogenomics in lung cancer: a review for the clinician. *Lung Cancer* 2018; 115: 34–41.
22. Safieh M, Korczyn AD and Michaelson DM. ApoE4: an emerging therapeutic target for Alzheimer's disease. *BMC Med* 2019; 17: 64.
23. Goerlich KS, Votinov M, Dicks E, *et al.* Neuroanatomical and neuropsychological markers of amnestic MCI: a three-year longitudinal study in individuals unaware of cognitive decline. *Front Aging Neurosci* 2017, 9: 34.
24. Genin E, Hannequin D, Wallon D, *et al.* APOE and Alzheimer disease: a major gene with semi-dominant inheritance. *Mol Psychiatry* 2011; 16: 903–907.
25. Sun R, Limkin EJ, Vakalopoulou M, *et al.* A radiomics approach to assess tumour-infiltrating CD8 cells and response to anti-PD-1 or anti-PD-L1 immunotherapy: an imaging biomarker, retrospective multicohort study. *Lancet Oncol* 2018; 19: 1180–1191.
26. Wu J, Aguilera T, Shultz D, *et al.* Early-stage non-small cell lung cancer: quantitative imaging

characteristics of ^{18}F Fluorodeoxyglucose PET/CT allow prediction of distant metastasis. *Radiology* 2016; 281: 270–278.

27. John A. Computational anatomy with the SPM software. *Magn Reson Imaging* 2009; 27: 1163–1174.
28. De Jay N, Papillon-Cavanagh S, Olsen C, *et al.* MRMRe: an R package for parallelized mRMR ensemble feature selection. *Bioinformatics* 2013; 29: 2365–2368.
29. Alshamlan H, Badr G and Alohali Y. mRMR-ABC: a hybrid gene selection algorithm for cancer classification using microarray gene expression profiling. *Biomed Res Int* 2015; 2015: 604910.
30. Xiang ZJ, Wang Y and Ramadge PJ. Screening tests for lasso problems. *IEEE Trans Pattern Anal Mach Intell* 2017; 39: 1008–1027.
31. Wu Y, Xu L, Yang P, *et al.* Survival prediction in high-grade osteosarcoma using radiomics of diagnostic computed tomography. *EbioMedicine* 2018; 34: 27–34.
32. Klöppel S, Stonnington CM, Chu C, *et al.* Automatic classification of MR scans in Alzheimer's disease. *Brain* 2008; 131: 681–689.
33. Teipel SJ, Born C, Ewers M, *et al.* Multivariate deformation-based analysis of brain atrophy to predict Alzheimer's disease in mild cognitive impairment. *NeuroImage* 2007; 38: 13–24.
34. Veitch DP, Weiner MW, Aisen PS, *et al.* Alzheimer's disease neuroimaging initiative. Understanding disease progression and improving Alzheimer's disease clinical trials: recent highlights from the Alzheimer's disease neuroimaging initiative. *Alzheimers Dement* 2019; 15: 106–152.
35. Tan C-C, Yu J-T and Tan L. Biomarkers for preclinical Alzheimer's disease. *J Alzheimers Dis* 2014; 42: 1051–1069.
36. Márquez F and Yassa MA. Neuroimaging biomarkers for Alzheimer's disease. *Mol Neurodegener* 2019; 14: 21.
37. Bozzali M, Serra L and Cercignani M. Quantitative MRI to understand Alzheimer's disease pathophysiology. *Curr Opin Neurol* 2016, 29: 437–444.
38. Chandra A, Dervenoulas G and Politis M; Alzheimer's Disease Neuroimaging Initiative. Magnetic resonance imaging in Alzheimer's disease and mild cognitive impairment. *J Neurol* 2019, 266: 1293–1302.
39. Fjell AM, McEvoy L, Holland D, *et al.* What is normal in normal aging? Effects of aging, amyloid and Alzheimer's disease on the cerebral cortex and the hippocampus. *Prog Neurobiol* 2014; 117: 20–40.
40. Axelrud LK, Santoro ML, Pine DS, *et al.* Polygenic risk score for Alzheimer's disease: implications for memory performance and hippocampal volumes in early life. *Am J Psychiatry* 2018, 175: 555–563.
41. Pini L, Pievani M, Bocchetta M, *et al.* Brain atrophy in Alzheimer's disease and aging. *Ageing Res Rev* 2016; 30: 25–48.
42. Shu Z-Y, Shao Y, Xu Y-Y, *et al.* Radiomics nomogram based on MRI for predicting white matter hyperintensity progression in elderly adults. *J Magn Reson Imaging* 2020; 51: 535–546.
43. Feng Q, Wang M, Song Q, *et al.* Correlation between hippocampus MRI radiomic features and resting-state intrahippocampal functional connectivity in Alzheimer's disease. *Front Neurosci* 2019; 13: 435.
44. Montembeault M, Brambati SM, Lamari F, *et al.* Atrophy, metabolism and cognition in the posterior cortical atrophy spectrum based on Alzheimer's disease cerebrospinal fluid biomarkers. *Neuroimage Clin* 2018; 20: 1018–1025.
45. Dickerson BC and Sperling RA. Neuroimaging biomarkers for clinical trials of disease-modifying therapies in Alzheimer's disease. *NeuroRx* 2005; 2: 348–360.
46. Bondi MW, Edmonds EC and Salmon DP. Alzheimer's disease: past, present, and future. *J Int Neuropsychol Soc* 2017; 23: 818–831.
47. Sevigny J, Chiao P, Bussière T, *et al.* The antibody aducanumab reduces Aβ plaques in Alzheimer's disease. *Nature* 2016; 537: 50–56.
48. Basaia S, Agosta F, Wagner L, *et al.* Alzheimer's disease neuroimaging initiative. Automated classification of Alzheimer's disease and mild cognitive impairment using a single MRI and deep neural networks. *Neuroimage Clin* 2019; 21: 101645.
49. Rafii MS. Tau PET imaging for staging of Alzheimer's disease in down syndrome. *Dev Neurobiol* 2019; 79: 711–715.
50. Schott JM, Kennedy J and Fox NC. New developments in mild cognitive impairment and Alzheimer's disease. *Curr Opin Neurol* 2006; 19: 552–558.

51. Encinas M, De Juan R, Marcos A, *et al.* Regional cerebral blood flow assessed with 99mTc-ECD SPET as a marker of progression of mild cognitive impairment to Alzheimer's disease. *Eur J Nucl Med Mol Imaging* 2003; 30: 1473–1480.

52. Chen J, Chen G, Shu H, *et al.* Predicting progression from mild cognitive impairment to Alzheimer's disease on an individual subject basis by applying the CARE index across different independent cohorts. *Aging* 2019; 11: 2185–2201.

53. Minhas S, Khanum A, Riaz F, *et al.* Predicting progression from mild cognitive impairment to Alzheimer's disease using autoregressive modelling of longitudinal and multimodal biomarkers. *IEEE J Biomed Health Inform* 2018; 22: 818–825.

54. Petersen RC, Thomas RG, Grundman M, *et al.* Vitamin E and donepezil for the treatment of mild cognitive impairment. *N Engl J Med* 2005; 352: 2379–2388.

55. Mitchell AJ and Shiri-Feshki M. Temporal trends in the long term risk of progression of mild cognitive impairment: a pooled analysis. *J Neurol Neurosurg Psychiatry* 2008; 79: 1386–1391.